Glycoconj J (2007) 24:33–47
DOI 10.1007/s10719-006-9010-3

Characterization of the N-linked oligosaccharides from human chorionic gonadotropin expressed in the methylotrophic yeast *Pichia pastoris*

Véronique Blanchard · Rupali A. Gadkari · Gerrit J. Gerwig · Bas R. Leeflang · Rajan R. Dighe · Johannis P. Kamerling

Abstract Human chorionic gonadotropin (hCG) is a heterodimeric, placental glycoprotein hormone involved in the maintenance of the corpus luteum during the first trimester of pregnancy. Biologically active hCG has been successfully expressed in the yeast *Pichia pastoris* (phCG). In the context of structural studies and therapeutic applications of phCG, detailed information about its glycosylation pattern is a prerequisite. To this end N-glycans were released with peptide-N^4-(N-acetyl-β-glucosaminyl)asparagine amidase F and fractionated via anion-exchange chromatography (Resource Q) yielding both neutral (80%) and charged, phosphate-containing (20%) high-mannose-type structures. Subfractionations were carried out via normal phase (Lichrosorb-NH_2) and high-pH anion-exchange (CarboPac PA-1) chromatography. Structural analyses of the released N-glycans were carried out by using HPLC profiling of fluorescent 2-aminobenzamide derivatives, MALDI-TOF mass spectrometry, and 500-MHz ^{1}H-NMR spectroscopy. Detailed neutral oligosaccharide structures, in the range of $Man_8GlcNAc_2$ to $Man_{11}GlcNAc_2$ including molecular isomers, could be established, and structures up to $Man_{15}GlcNAc_2$ were indicated. Phosphate-containing oligosaccharides ranged from $Man_9PGlcNAc_2$ to $Man_{13}PGlcNAc_2$. Mannosyl O-glycans were not detected. Profiling studies carried out on different production batches showed that the oligosaccharide structures are similar, but their relative amounts varied with the culturing media.

Keywords Glycosylation · *Pichia pastoris* · Human chorionic gonadotropin · High-mannose-type N-glycans · Phosphorylation

Abbreviations

hCG	human chorionic gonadotropin
phCG	human chorionic gonadotropin expressed in *Pichia pastoris*
uhCG	urinary human chorionic gonadotropin
PNGase F	peptide-N^4-(N-acetyl-β-glucosaminyl) asparagine amidase F
FPLC	fast protein liquid chromatography
2AB	2-aminobenzamide
MALDI-TOF-MS	matrix-assisted laser desorption ionization time-of-flight mass spectrometry
HPLC	high-performance liquid chromatography
HPAEC	high-pH anion-exchange chromatography
PAD	pulsed amperometric detection
TOCSY	total correlation spectroscopy
ROESY	rotating-frame nuclear Overhauser enhancement spectroscopy
WEFT	water eliminated Fourier transform
MLEV	composite pulse devised by M. Levitt

Introduction

The placental glycoprotein hormone human chorionic gonadotropin (hCG), excreted in the urine, plays a major

---

V. Blanchard · G. J. Gerwig · B. R. Leeflang · J. P. Kamerling (✉)
Bijvoet Center, Department of Bio-Organic Chemistry,
Utrecht University, Padualaan 8,
NL-3584 CH Utrecht, The Netherlands
e-mail: j.p.kamerling@chem.uu.nl

R. A. Gadkari · R. R. Dighe
Department of Molecular Reproduction,
Development and Genetics, Indian Institute of Science,
Bangalore 560012, India

role during the first trimester of pregnancy. It indirectly stimulates the corpus luteum to produce progesterone until the placenta itself acquires the ability to produce this pregnancy-sustaining steroid [1]. Usually, hCG isolated from the urine of pregnant women is used in the *in vitro* fertilization technology as a therapeutic analogue of lutropin for the induction of final follicular maturation and ovulation in infertile women.

Native hCG consists of two non-covalently associated subunits, denoted α and β, and is glycosylated for about 30%. The α-subunit (~15 kDa), containing 92 amino acids, is N-glycosylated at Asn52 and Asn78, and the β-subunit (~23 kDa), consisting of 145 amino acids, is N-glycosylated at Asn13 and Asn30 and O-glycosylated at Ser121, Ser127, Ser132, and Ser138. The distribution of the N-glycans on urinary hCG was found to be site-specific [2–4]: monosialylated monoantennary and disialylated diantennary structures, with Neu5Ac in (α2–3) linkage to Gal, were found at all N-glycosylation sites whereas monosialylated hybrid-type structures only occur at α-hCG Asn52 and (α1–6)-fucosylation only at β-hCG Asn13 and Asn30. Indications for the occurrence of trisialylated tri- and tri′-antennary glycans on β-hCG have also been reported [5]. Structural data for the O-glycosylation comprise mainly the conventional mono- and disialylated core 1-type structures, the disialyl-hexasaccharide (including core 2 type), and the sialylated disaccharide [6–8]. A random distribution of these O-glycans among the attachment sites has been suggested [9]. Over the years many studies have appeared demonstrating the crucial importance of the glycosylation of hCG for its biological functioning (for a review, see e.g., [10]). In reaching conclusions, site-directed mutagenesis of specific (glycosylation) sites in urinary hCG applying different host cell systems played a major role.

In order to replace for pharmaceutical applications the urinary glycohormone by a recombinant variant, detailed attention has to be paid to the glycosylation patterns generated in relevant host cell systems. Expression of hCG in CHO cells shows the same mono-, di-, tri-, and tri′-antennary N-glycans as found for urinary hCG; Neu5Ac occurs in (α2–3) linkage to Gal. The O-glycans comprise mainly the convential saccharides (see above) [8, 11, 12]. CHO cells have also been used for generating ^{13}C/^{15}N-labeled hCG for NMR studies [13]. Expression of hCG in baculovirus insect cell systems yields hCG which appears to have also oligomannose-type chains [14–16]. Furthermore, oligomannose-type chains were found on hCG expressed in *Dictyostelium discoideum* [17, 18]. Expression of hCG in malignant trophoblastic JAR cells yielded a β-subunit with predominantly endo-H-resistant N-glycans and an α-subunit with a more complicated array of endo-H-resistant and endo-H-sensitive (hybrid) N-glycans [19, 20]. Recombinant hCG from mouse C127 mammary tumor cells showed that, compared with urinary hCG, only the α-subunit has strongly deviating glycans; i.e., sialylated diantennary chains were suggested to be replaced by not-specified sialylated triantennary chains [21].

In earlier studies it has been shown that the methylotrophic yeast *Pichia pastoris* allows an easy production of biologically active hCG [22, 23]. However, *P. pastoris* does not produce the typical oligomannose-, hybrid- and complex-type glycosylation patterns as generally found in mammalian cell systems. Several studies on other recombinant glycoproteins expressed in *P. pastoris* have shown that relatively small (compared with glycoproteins from other yeast species) (phosphorylated) high-mannose-type structures are present, generally containing 8 to 14 Man residues [24–28]. O-Mannosylation of proteins expressed in *P. pastoris* has also been reported (1–5 mannose residues) [29–32]; however, it occurs less frequently than N-glycosylation.

In the context of broader studies focused on the pharmaceutical use of *P. pastoris* expressed hCG (phCG) and on the use of *P. pastoris* cells to prepare ^{13}C/^{15}N-labeled phCG for three-dimensional studies of its structure in solution using NMR spectroscopy, a detailed glycan analysis of phCG was undertaken by mass spectrometry and NMR spectroscopy. In addition, attention was paid to possible changes in glycosylation pattern when changing the culturing conditions.

Materials and methods

Recombinant hCG expressed in *Pichia pastoris* (phCG)

The cloning, expression, and purification of biologically active phCG have been described previously [23]. Briefly, PCR-amplified hCG was cloned into a pPIC9k expression vector, and the best phCG-secreting clone was selected and grown in a 10 liter fermenter vessel. The secreted protein was purified from the culture supernatant and its biological activity determined by RIA. Batch I was produced exactly according to [23]; ammonia was used as nitrogen source, and glycerol then methanol as carbon sources. Batch II was produced using FM22 medium (Invitrogen); ammonium sulfate was used as nitrogen source, and glycerol then methanol as carbon sources (to be published).

Monosaccharide analysis

Human phCG (400 μg) was desalted on a Pharmacia FPLC system using 5 HiTrap columns (5×5 ml) connected in series. The eluent consisted of 5 mM NH_4HCO_3 and the fractionation was monitored by UV detection at 214 nm. The sample was lyophilized, and subjected to methanolysis

(1.0 M methanolic HCl, 24 h, 85°C) followed by re-*N*-acetylation and trimethylsilylation [33]. The generated mixture of trimethylsilylated methyl glycosides was analyzed by GLC on an EC-1 column (30 m × 0.32 mm; Alltech, Breda, The Netherlands), using a Chrompack CP9002 gas chromatograph (temperature program 140–240°C at 4°C/min) and flame-ionization detection.

Reduction and carboxymethylation

Human phCG was reduced and *S*-carboxymethylated according to procedures described before [21]. Briefly, phCG (12 mg) was dissolved in 6.5 ml 1 M Tris/HCl, pH 8.25, containing 6 M guanidinium-HCl, 1 mM EDTA, and 34 mM dithiothreitol; and the solution was kept for 2 h at 37°C. Then, iodoacetic acid (0.5 M in 0.5 M NaOH) was added to a final concentration of 68 mM, and the incubation was continued for 30 min in the darkness. After quenching the reaction by adding an excess of 2-mercaptoethanol, low-molecular-mass compounds were removed by using 5-kDa centrifugal concentrators, and the retentate was lyophilized. The chemical conversion was checked by 10% SDS-PAGE under reducing conditions.

Separation of the subunits

For the N-glycan profiling studies on the α- and β-subunits of the phCG batches I and II, prior to digestion with peptide-N^4-(*N*-acetyl-β-glucosaminyl)asparagine amidase F (PNGase F; EC 3.5.1.52) (Roche Molecular Biochemicals, IN) and labeling with 2-aminobenzamide (2AB; Sigma), reduced and carboxymethylated phCG (2 mg) was separated into subunits on a Superdex G75 column (60 × 2.6 cm; Pharmacia, Uppsala, Sweden) using 50 mM NH_4HCO_3, pH 7.0, as eluent at a flow rate of 1 ml/min, monitored at 214 nm (Uvicord, LKB).

Release and isolation of N-glycans

Reduced and carboxymethylated phCG (batch I; ~12 mg) was dissolved in 6 ml 20 mM NaH_2PO_4/Na_2HPO_4, pH 7.2, containing 10 mM EDTA, and digested with 8 U of PNGase F for 24 h at 37°C. The N-glycan pool was separated from the protein on a Superdex G75 column using the same conditions as described above. N-Deglycosylated phCG and the pool of N-glycans were then lyophilized.

FPLC fractionation

The pool of N-glycans was fractionated according to charge on a Resource Q anion-exchange column (1 ml, Pharmacia) at a flow rate of 1 ml/min [6] using a Pharmacia FPLC system. The elution, monitored by UV absorbance at 214 nm, was performed with 4 ml H_2O, followed by a linear concentration gradient of 0–500 mM NaCl in 9 ml H_2O. The fractions obtained were desalted on Carbograph extract-clean columns (Alltech) [34], and lyophilized.

HPLC fractionation

The FPLC fractions were further fractionated on a Lichrosorb-NH_2 10 μm column (25 × 0.46 cm, Alltech) equipped with a LiChrospher Amino 5 μm guard column (7.5 × 4.6 mm), using a Waters 600 HPLC system. Elutions were performed with a linear gradient of 30 mM K_2HPO_4/KH_2PO_4, pH 6.8, in acetonitrile at a flow rate of 1 ml/min, and monitored by UV absorbance at 206 nm. Relevant fractions were concentrated under a N_2 stream, desalted on Carbograph extract-clean columns (Alltech), and lyophilized.

HPAEC fractionation

HPAEC was performed on a Dionex DX 500 system equipped with a pulsed amperometric detection (PAD) unit. Neutral oligosaccharide fractions were subfractionated on a CarboPac PA-1 column (4 × 250 mm) using a gradient of 0.5 M sodium acetate/0.1 M NaOH (solvent B) in 0.1 M NaOH (solvent A) at a flow rate of 1 ml/min. The samples were loaded in 2% B–98% A, then the proportion of B was increased to 15% in 15 min, and then to 20% in 17 min, 33% in 6 min, 100% in 2 min. After 5 min of isocratic elution, the solvent system was put back to the initial conditions and equilibrated for 10 min. Fractions were immediately neutralized with 0.1 M HCl, desalted on Carbograph extract-clean columns (Alltech), and lyophilized.

Modifications of the charged N-glycans

Mild acid treatment of glycans (1 μg) was carried out in 100 mM HCl (500 μl) for 30 min at 100°C [35]. Terminal phosphate groups attached to non-reducing ends of glycans were cleaved by treatment with 2 U alkaline phosphatase (Sigma, St. Louis, MO) in 50 mM citrate/phosphate buffer, pH 9, for 24 h at 37°C.

2AB-labeling of N-glycans and HPLC profiling

2AB-labeling of oligosaccharides was performed as described earlier [36, 37]. Briefly, about 1 nmol of dried glycans was incubated with 0.35 M 2-aminobenzamide/1 M sodium cyanoborohydride in acetic acid-dimethyl sulfoxide (3:7, v/v) (10 μl) for 2 h at 65°C. For the clean-up of the 2AB-labeled glycans, pre-treated (0.5% acetic acid for 24 h) quartz microfibre filters (QM-A, Whatman, England) were used. After applying the samples to a paper strip, the excess of reagents was removed by washing with 8 × 0.5 ml acetonitrile.

Glycans were eluted from the paper strip with 4×0.5 ml H_2O, and, after lyophilization, residues were dissolved in 200 µl H_2O.

Neutral N-glycan profiling was conducted by HPLC on a normal phase TSKgel Amide-80 column (4.6×250 mm; Tosoh BioScience, Germany), using a Waters 2690 XE Alliance System, equipped with a Waters 474 scanning fluorescence detector ($\lambda_{exc\cdot max}$=373 nm, $\lambda_{em\cdot max}$=420 nm). For the elution, two solvent systems were used: solvent A, 50 mM ammonium formate, pH 4.4-acetonitrile (1:4, v/v); solvent B, 50 mM ammonium formate, pH 4.4. The linear gradients were comprised of 6.5 to 43.8% B in 100 min, followed by 43.8 to100% B over the next 3 min, then 100% B for 5 min before returning to the initial conditions in 5 min. The total run time at a flow rate of 0.8 ml/min was 140 min. Elution positions of the 2AB-labeled glycans were standardized in glucose units (GU) using a 2AB-labeled partial dextran hydrolysate as reference [38, 39].

Charged N-glycan profiling was performed by HPLC on a weak anion-exchange Vydac 301 VHP5410 column (4.6× 100 mm; Grace Vydac, Hesperia, CA), using the same equipment as above. For the elution, two solvent systems were used: solvent A, 20% acetonitrile; solvent B, 0.5 M ammonium formate, pH 4.4-H_2O-acetonitrile (5:3:2, v/v). After running 100% A for 5 min, charged N-glycans were eluted with a linear gradient of 0 to 100% B over 35 min. 100% B was maintained for 5 min before returning to the initial conditions in 1 min followed by a reequilibration step of 14 min. The total run time at a flow rate of 0.4 ml/min was 60 min.

Matrix-assisted laser desorption ionization time-of-flight mass spectrometry

MALDI-TOF mass spectra were recorded on a Voyager-DE mass spectrometer (Applied Biosystems) with implemented delayed extraction technique, equipped with a N_2 laser (337 nm, 3 ns pulse width). Spectra were recorded in a linear mode at an accelerating voltage of 24.5 kV using an extraction delay of 90 ns. For measurements in the positive-ion mode, 0.5-µl samples were mixed in a 1:1 ratio on the target with 2,5-dihydroxybenzoic acid (10 mg/ml) dissolved in H_2O-ethanol (9:1, v/v). For measurements in the negative-ion mode, 2′,4′,6′-trihydroxyacetophenone (10 mg/ml) dissolved in acetonitrile −20 mM ammonium citrate (1:1, v/v) was used as a matrix. In this case, the samples were dried under reduced pressure [40].

^{1}H-NMR spectroscopy

^{1}H-NMR spectra were recorded on a Bruker AMX-500 spectrometer (Bijvoet Center, Department of NMR Spectroscopy, Utrecht University) at a probe temperature of 27°C and p^{2}H 7. Samples were dissolved in 500 µl 99.9% ^2H_2O (Cambridge Isotope Laboratories Inc., Andover, MA). Chemical shifts (δ) are expressed in ppm by reference to internal acetone (δ 2.225 in ^2H_2O) [41]. HOD signal suppression was performed by applying a WEFT pulse sequence in 1D experiments [42] and by a pre-saturation of 1 s during the relaxation delay in 2D experiments. 2D-TOCSY spectra were recorded using MLEV-17 mixing sequence cycles of 50 ms, 2D-ROESY spectra were recorded with a mixing time of 300 ms, and 2D-NOESY spectra with a mixing time of 500 ms. NMR data sets were processed using in house developed software packages (J.A. van Kuik, Bijvoet Center, Department of Bio-Organic Chemistry, Utrecht University).

Results

Monosaccharide analysis [33] of phCG revealed a carbohydrate content of 30% (by mass) and the presence of mannose and *N*-acetylglucosamine in the molar ratio of 9:2. After reduction and carboxymethylation, phCG was digested with PNGase F, whereby SDS-PAGE was used to check the completeness of the de-N-glycosylation. The released pool of N-glycans, isolated via size-exclusion chromatography on Superdex G75, was fractionated by anion-exchange chromatography on Resource Q (FPLC), yielding three carbohydrate-containing fractions eluting at positions corresponding to neutral (**Q0**; 80%) and charged (**Q1**; 15% /**Q2**; 5%) compounds (Fig. 1), as calculated from UV peak areas.

Neutral oligosaccharides

The pool of neutral N-glycans **Q0** was analyzed in terms of molecular mass by MALDI-TOF-MS. In Fig. 2a its

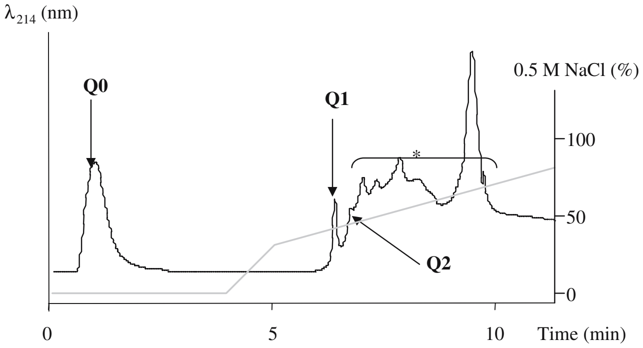

Fig. 1 Fractionation pattern of PNGase F-released phCG N-glycans at 214 nm on a FPLC Resource Q anion-exchange column. Elutions were performed at a flow rate of 1 ml/min with a gradient of NaCl in H_2O as shown in the figure. The fraction marked by an asterisk did not contain any carbohydrate material

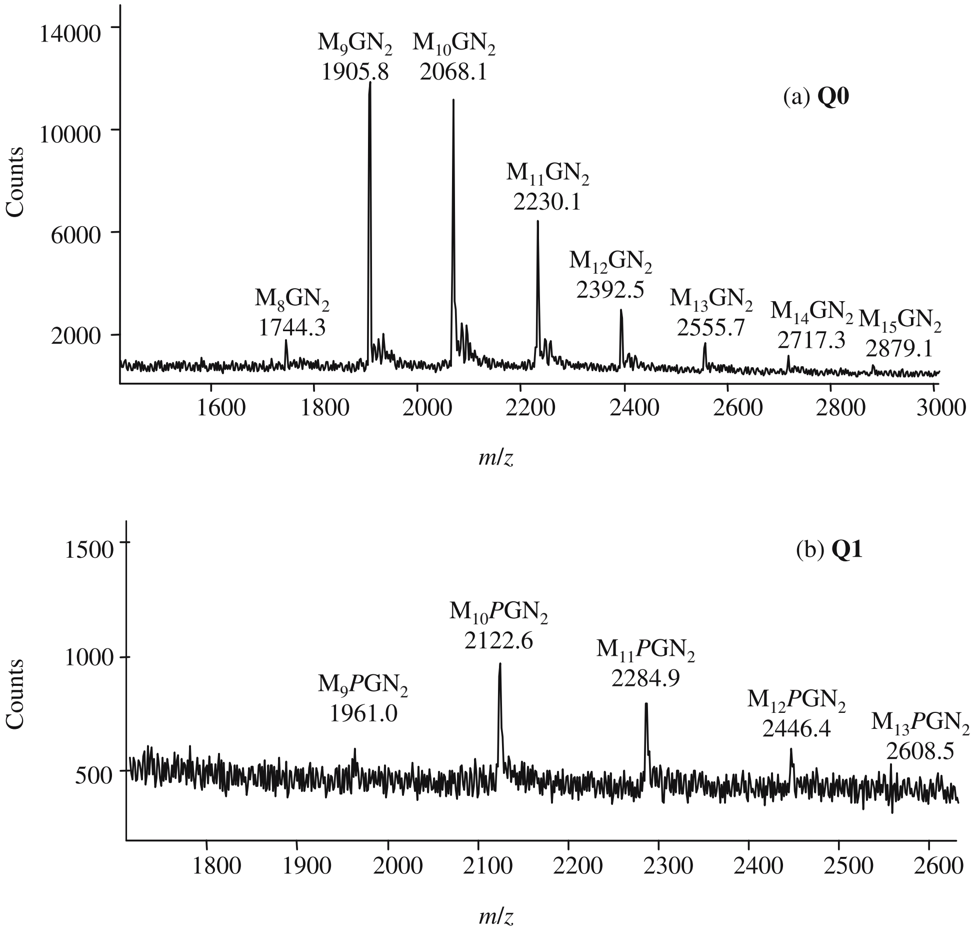

Fig. 2 MALDI-TOF mass spectra: (a) neutral fraction **Q0**, positive-ion mode, $[M + Na]^+$; (b) charged fraction **Q1**, negative-ion mode, $[M - H]^-$. M=Man; GN=GlcNAc; *P*=phosphate

positive-ion mode mass spectrum is depicted, showing that the compounds range from $Man_8GlcNAc_2$ to Man_{15}-$GlcNAc_2$ (**Q0.M8** to **Q0.M15**). The HPLC profile (normal phase TSKgel Amide-80) of the pool of N-glycans **Q0**, labeled with 2-aminobenzamide (2AB derivatives), is in agreement with the presence of $Man_8GlcNAc_2$ to Man_{12}-$GlcNAc_2$ (Fig. 3). The presence of various structural isomers of the higher mass components (see below) can be held responsible for the not-well resolved HPLC pattern from $Man_{10}GlcNAc_2$ on. Fractionation of FPLC fraction **Q0** by normal-phase HPLC on Lichrosorb-NH_2 yielded five subfractions (Fig. 4a), which were analyzed by MALDI-TOF-MS to show that in terms of molecular mass pure $Man_8GlcNAc_2$ (11%), $Man_9GlcNAc_2$ (47%), Man_{10}-$GlcNAc_2$ (28%), $Man_{11}GlcNAc_2$ (10%), and $Man_{12}GlcNAc_2$ (4%) oligosaccharides were obtained. The $Man_8GlcNAc_2$ to $Man_{12}GlcNAc_2$ subfractions (**Q0.M8-Q0.M12**) were further investigated by 500-MHz 1D and 2D ^{1}H-NMR spectroscopy. When necessary, additional fractionations were carried out with HPAEC-PAD on CarboPac PA-1. A summary of the established structures is presented in Scheme 1. The ^{1}H-chemical shifts of the H-1 and H-2 protons of the constituent monosaccharides of the reported structures are listed in Table 1. The ^{1}H-NMR data of $Man_xGlcNAc_1$ (x = 9 − 11) [25, 43] were partly used to assign the N-glycans of phCG.

$Man_8GlcNAc_2$ pool

The structural-reporter-group region of the ^{1}H-NMR spectrum of subfraction **Q0.M8** indicated a homogeneous

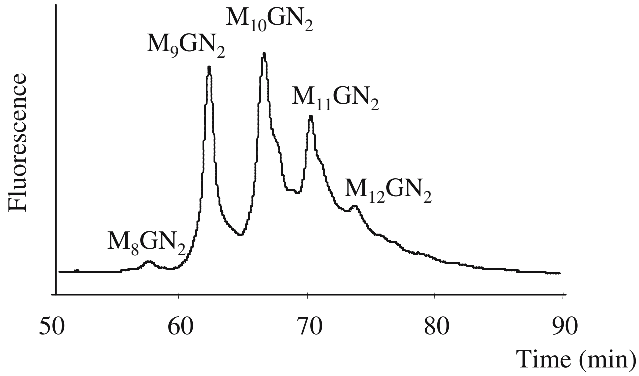

Fig. 3 HPLC profile of the fluorescent 2AB-labeled neutral oligosaccharide pool **Q0** on a normal-phase TSKgel Amide-80 column. Elutions were carried out at a flow rate of 0.8 ml/min with a gradient of ammonium formate, pH 4.4, in acetonitrile (see Materials and methods). M=Man; GN=GlcNAc

Fig. 4 HPLC elution profile at 206 nm on Lichrosorb-NH_2 of (a) fraction **Q0** and (b) fraction **Q1**. Elutions were performed at a flow rate of 1 ml/min with a linear gradient of 30 mM phosphate buffer, pH 6.8, in acetonitrile. M=Man; GN=GlcNAc

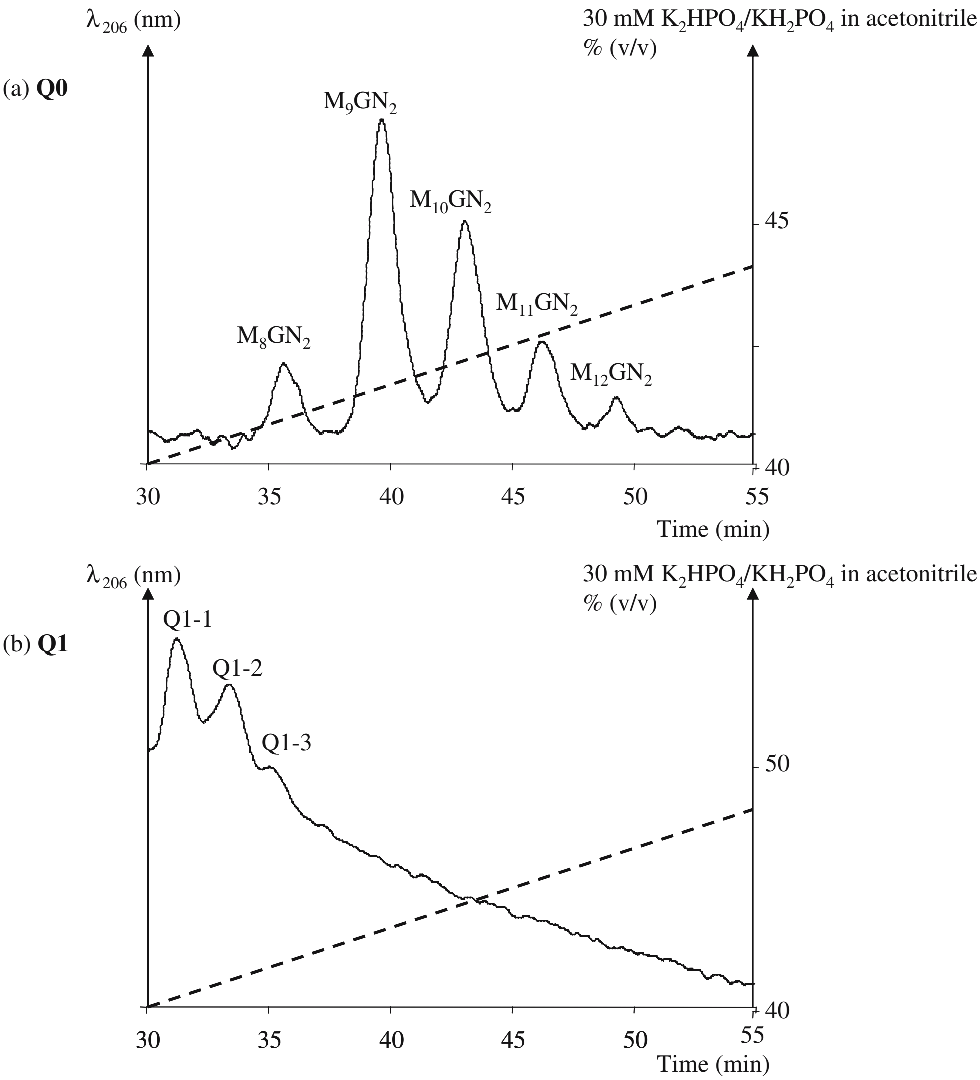

$Man_8GlcNAc_2$ isomer, missing the Man-$\mathbf{D_2}$ residue (Fig. 5a, Scheme 1, Table 1). The Man H-1 and H-2 chemical shifts are in agreement with literature data for this structure (see e.g., glycan QN2.4 of the human epidermal growth factor receptor [37]). For comparison with ^{1}H-NMR data of the isomers missing the Man-$\mathbf{D_1}$ or Man-$\mathbf{D_3}$ residue, see [44] and [45], respectively. For comparison with ^{1}H-NMR data of $Man_9GlcNAc_2$, containing Man-$\mathbf{D_1}$, Man-$\mathbf{D_2}$, and Man-$\mathbf{D_3}$, see [46]. The identified isomer, reflecting the usual first steps in trimming $Glc_3Man_9GlcNAc_2$ of N-glycans, has been reported to be an essential intermediate in yeast oligosaccharide processing [27, 47].

$Man_9GlcNAc_2$ pool

The structural-reporter-group region of the ^{1}H-NMR spectrum of subfraction **Q0.M9** revealed the presence of two $Man_9GlcNAc_2$ isomers, **Q0.M9-1** and **Q0.M9-2**, with **Q0.M9-1** as the major component (Fig. 5b, Scheme 1, Table 1). The structure of **Q0.M9-1** was identified as an extension of the $Man_8GlcNAc_2$ structure with a Man-**C′** residue, (α1–6)-linked with Man-**4**, thereby creating the typical yeast-processed $Man_9GlcNAc_2$ structure. Compared with the ^{1}H-NMR spectrum of **Q0.M8**, the spectrum of **Q0.M9** shows two additional structural-reporter-group signals, an H-1 signal at δ 4.927 and an H-2 signal at δ 3.99, both characteristic of terminal Man-**C′** in a Man-**C′**-(α1–6)-Man-**4** element [25, 43]. Going from **Q0.M8** to **Q0.M9-1**, shifts are observed for Man-**A** H-1 (δ 5.088 vs 5.099) and Man-**3** H-2 (δ 4.23 vs 4.16). Interestingly, the Man-$\mathbf{D_1}$ and Man-$\mathbf{D_3}$ H-1 signals are split, and it is suggested that, due to the extension of $Man_8GlcNAc_2$ with Man-**C′**, Man-$\mathbf{D_1}$ H-1 shifts a little bit. By integration of the spectrum, it was concluded that this isomer represents about 95% of the total $Man_9GlcNAc_2$ pool. The low-intense H-1 signal (5%) at δ 5.404, representing a Man-**A** residue extended with a Man-$\mathbf{D_2}$ residue, and the

Man-**3** H-2 signal (5%) at δ 4.23 [41, 46, 48], support the presence of structure **Q0.M9-2**, the convential precursor Man$_9$GlcNAc$_2$ structure formed in the oligosaccharide processing of Glc$_3$Man$_9$GlcNAc$_2$.

Man$_{10}$GlcNAc$_2$ pool

The structural-reporter-group region of the ^{1}H-NMR spectrum of subfraction **Q0.M10** indicated the presence of a mixture of Man$_{10}$GlcNAc$_2$ isomers (Fig. 5c, Scheme 1, Table 1). For Man-**A** two H-1 signals were found: a very minor one corresponding with a Man-**A** residue bearing a Man-$\mathbf{D_2}$-(α1–2) residue (H-1, δ 5.404), and a major one reflecting a terminal Man-**A** residue (H-1, δ 5.100). As a consequence, the very minor Man$_{10}$GlcNAc$_2$ isomer is an extension of **Q0.M9-2** (not assigned), and the major Man$_{10}$GlcNAc$_2$ isomers are extensions of **Q0.M9-1**, which means potential extensions at Man-$\mathbf{D_3}$, Man-$\mathbf{D_1}$, or Man-**C′**. Man(α1–3) extensions at Man-$\mathbf{D_1}$ and Man-$\mathbf{D_3}$, as reported for yeast glycans from *Saccharomyces cerevisiae* (see compounds M$_{11}$ and M$_{13}$ in [49]) could be eliminated by inspection of 2D TOCSY spectra of **Q0.M10**: no H-1,H-2 correlation was found at δ 5.144/4.23. This finding is in accordance with the deficiency of the α-1,3-mannosyltransferase responsible for outer (α1–3)-mannosylations in *P. pastoris* as compared to *S. cerevisiae* [25]. Comparing the ^{1}H-NMR spectra of **Q0.M9** and **Q0.M10** shows various changes in intensities of H-1 signals and new H-1 signals are observed at δ 4.912 and 5.121.

The Man$_{10}$GlcNAc$_2$ pool was further fractionated by HPAEC (Fig. 6a), and three subfractions were isolated, **Q0.M10-1**, **Q0.M10-2**, and **Q0.M10-3**, which were checked by MALDI-TOF-MS to be pure Man$_{10}$GlcNAc$_2$ isomers. Subfraction **Q0.M10-3** did not contain sufficient material for NMR analysis.

The ^{1}H-NMR spectrum of HPAEC subfraction **Q0.M10-1** revealed the presence of two isomeric structures, compounds **Q0.M10-1a** and **Q0.M10-1b** (Fig. 7a, Scheme 1, Table 1), in agreement with the HPAEC peak pattern (Fig. 6a). The relatively high intensities of the structural-reporter-group H-1 signals at δ 5.303 [internal Man unit in Man-(α1–2)-Man-(α1- element] and 5.049 [terminal Man unit in Man-(α1–2)-Man-(α1- element] indicated that the Man$_{10}$GlcNAc$_2$ isomers have the structure **Q0.M9-1** with an extra (α1–2)-linked Man residue. The unusual low intensity of the Man-**B** H-1 signal (δ 5.144) might be due to a change in local mobility of this proton. The H-1 signal at δ 5.121 was assigned to Man-**C′** when substituted with

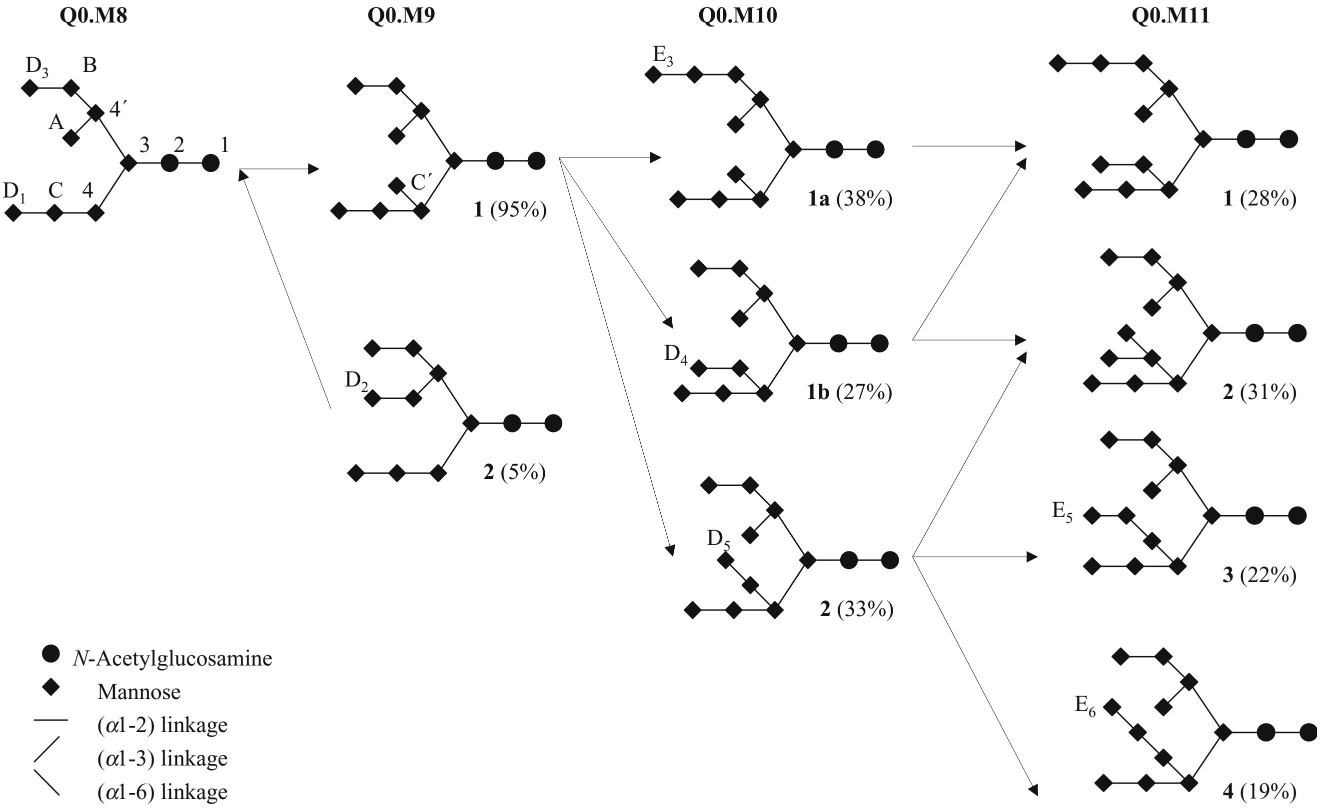

Scheme 1 N-linked oligosaccharide structures isolated from phCG. Note that the possible occurrence of Man-$\mathbf{E_3}$ at Man-$\mathbf{D_1}$ has not been excluded (see text)

Table 1 ^{1}H-chemical shifts data of the structural-reporter-group protons of the high-mannose-type N-glycans derived from phCG

Reporter group	Residue	Chemical shift in ppm										
		Q0									**Q1**	
		M8	**M9-1**	**M10-1a**	**M10-1b**	**M10-2**	**M11-1**	**M11-2**	**M11-3**	**M11-4**	**1**	**2**
H-1	GlcNAc-**1α**	5.188	5.188	5.190	5.190	5.190	5.189	5.189	5.190	5.190	5.190	5.190
	GlcNAc-**1β**	n.d.	4.867	n.d.	n.d.	n.d.	n.d.	n.d.	n.d.	n.d.	n.d.	n.d.
	GlcNAc-**2**	4.60	4.60	4.60	4.60	4.60	4.60	4.60	n.d.	n.d.	4.60	4.60
	Man-**3**	n.d.	n.d.	n.d.	n.d.	n.d.	n.d.	n.d.	n.d.	n.d.	n.d.	n.d.
	Man-**4**	5.339	5.341	5.342	5.342	5.342	5.339	5.344	5.344	5.343	5.338	5.338
	Man-**4′**	4.870	4.871	4.871	4.871	4.871	4.869	4.870	4.868	4.870	4.871	4.870
	Man-**A**	5.088	5.099	5.100	5.100	5.100	5.098	5.097	5.097	5.097	5.086	5.086
	Man-**B**	5.146	5.145	5.144	5.144	5.144	5.142	5.145	5.143	5.143	5.144	5.141
	Man-**C**	5.304	5.303	5.303	5.303	5.303	5.302	5.302	5.301	5.302	5.303	5.305
	Man-**C′**	–	4.927	4.927	5.121	4.912	5.121	5.122	4.911	4.91	4.928	4.912
	Man-**D**$_1$	5.043	5.047	5.049	5.049	5.049	5.049	5.049	5.049	5.047	5.048	5.049
	Man-**D**$_3$	5.043	5.043	5.303	5.049	5.042	5.302	5.049	5.049	5.047	5.048	5.049
	Man-**D**$_4$	–	–	–	5.049	–	5.049	5.049	–	–	–	–
	Man-**D**$_5$	–	–	–	–	4.912	–	4.929	5.121	4.91	–	4.912
	Man-**E**$_3$	–	–	5.049	–	–	5.049	–	–	–	–	–
	Man-**E**$_5$	–	–	–	–	–	–	–	5.049	–	–	–
	Man-**E**$_6$	–	–	–	–	–	–	–	–	4.91	–	–
	Man-*P*										5.439 5.414	5.439 5.411 5.450
H-2	Man-**3**	4.23	4.16	4.16	4.16	4.16	n.d.	n.d.	n.d.	n.d.	n.d.	
	Man-**4**	4.09	4.09	4.09	4.09	4.09	4.09	4.09	4.09	4.09	4.09	
	Man-**4′**	4.14	4.15	4.15	4.15	4.15	4.15	4.15	4.15	4.15	4.14	
	Man-**A**	4.07	4.07	4.07	4.07	4.07	4.07	4.07	4.07	4.07	4.07	
	Man-**B**	4.04	4.03	4.03	4.03	4.03	4.02	4.02	4.02	4.02	4.03	
	Man-**C**	4.11	4.12	4.11	4.11	4.11	4.11	4.11	4.11	4.11	4.11	
	Man-**C′**	–	3.99	4.00	4.02	3.99	4.02	4.02	3.99	3.99	3.99	
	Man-**D**$_1$	4.07	4.07	4.07	4.07	4.07	4.07	4.07	4.07	4.07	4.07	
	Man-**D**$_3$	4.07	4.07	4.11	4.07	4.07	4.11	4.07	4.07	4.07	4.07	
	Man-**D**$_4$	–	–	–	4.07	–	4.07	4.07	–	–	–	
	Man-**D**$_5$	–	–	–	–	3.99	–	3.99	4.02	3.99	–	
	Man-**E**$_3$	–	–	4.07	–	–	4.07	–	–	–	–	
	Man-**E**$_5$	–	–	–	–	–	–	–	4.07	–	–	
	Man-**E**$_6$	–	–	–	–	–	–	–	–	3.99	–	
	Man-*P*										4.00 3.98	

Chemical shifts are given relative to internal acetone (δ 2.225) in ^2H_2O at 300 K and at p^{2}H 7 [41]. n.d. = not determined

a Man(α1–2) residue (see ^{1}H-NMR data of Man$_{10}$GlcNAc$_1$ compound IIIa in [25]). Consequently, compound **Q0.M10-1b** can be formulated as an extension of **Q0.M9-1** with a Man-**D**$_4$ residue at Man-**C′**. Taking into account the terminal position of Man-**A** (H-1, δ 5.100; see above) and the fact that Man-**C′** also occurs in terminal position (H-1, δ 4.927), remaining linear extensions can only take place at Man-**D**$_1$ or Man-**D**$_3$ of **Q0.M9-1**. Previously, based on NMR studies carried out at 23°C, it has been reported for Man$_{10}$GlcNAc$_1$ that in *P. pastoris* extensions occur preferably at Man-**D**$_3$ and not at Man-**D**$_1$ [25]. This choice was based on differences in Man-**4** H-1 values comparing the Man-**D**$_1$-(α1–2)-Man-**C**-(α1–2)-Man-**4** and Man-**C**-(α1–2)-Man-**4** sequences in Man$_8$GlcNAc$_1$ at 70°C (Man-**4** H-1, $\Delta\delta = -0.013$) (at 23°C the Man-**4** H-1 chemical shifts are identical) [47] and in Man$_{6/8}$GlcNAc-ol at 40°C (Man-**4** H-1, $\Delta\delta = -0.012$) [50]. Like the Man-**4** H-1 values of the three Man$_8$GlcNAc$_1$ isomers at 23°C, also those of the three Man$_8$GlcNAc$_2$ isomers have identical chemical shifts at 27°C [37, 44, 45]. Based on our NMR data of **Q0.M10-1**, obtained at 23, 27, 40, and 70°C, a definite choice for the extension of the additional Man residue, at Man-**D**$_3$

or at Man-$\mathbf{D_1}$, turned out to be not possible. For reasons of readability, in Scheme 1, the location of the additional (α1–2)-linked Man residue (Man-$\mathbf{E_3}$) has been set at Man-$\mathbf{D_3}$ (structure **Q0.M10-1a**); in Table 1 the assignments have also been arranged following an extension of Man-$\mathbf{D_3}$.

The ^{1}H-NMR spectrum of HPAEC subfraction **Q0.M10-2** is very similar to that of **Q0.M9-1** (Fig. 7b, Scheme 1, Table 1). Only the Man H-1,H-2 couple at δ 4.912/3.99 occurs with double intensity, indicating the presence of an extra Man residue with nearly identical structural reporters as Man-**C′**. As reported earlier, these signals have been shown to be characteristic for an (α1–6)-linked Man residue at Man-**C′** (Man-$\mathbf{D_5}$-(α1–6)-Man-**C′**-(α1–6)-Man-**4**) (see Man$_{10}$-GlcNAc$_1$ compound IIIc in [25]. As mentioned above for **Q0.M9-1**, also the spectrum of **Q0.M10-2** shows a minor separation of the Man-$\mathbf{D_1}$ and Man-$\mathbf{D_3}$ H-1 signals. The fact that **Q0.M10-2** has a higher HPAEC retention time than **Q0.M10-1a** and **Q0.M10-1b** is in agreement with the occurrence of one extra HO2 group in **Q0.M10-2** [25, 51, 52].

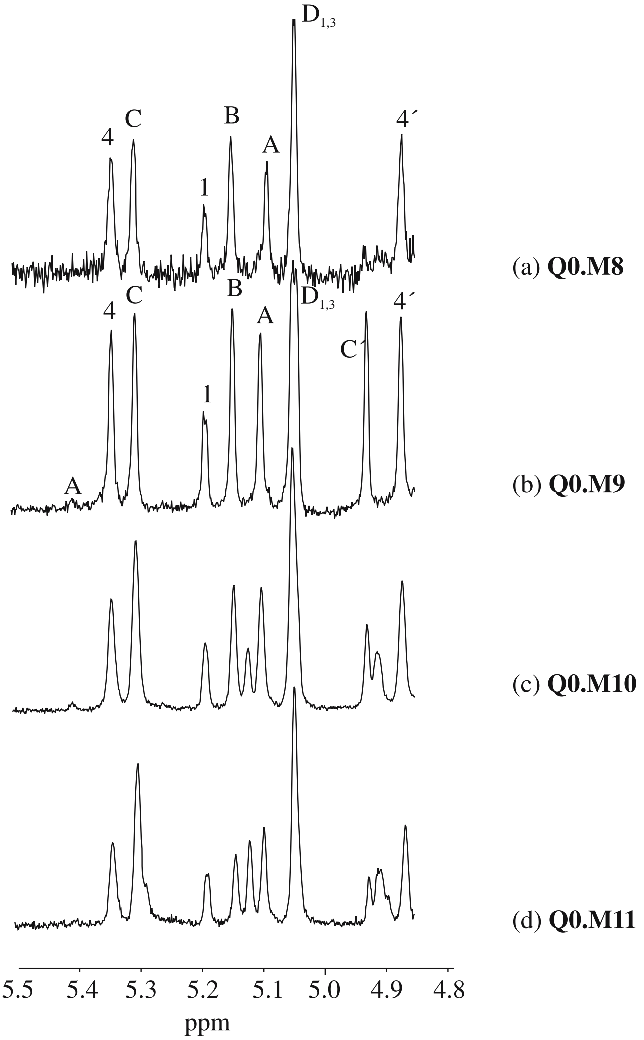

Fig. 5 Anomeric regions of ^{1}H-NMR spectra of neutral oligosaccharides (a) Man$_8$GlcNAc$_2$ (**Q0.M8**), (b) Man$_9$GlcNAc$_2$ (**Q0.M9**), (c) Man$_{10}$GlcNAc$_2$ (**Q0.M10**), and (d) Man$_{11}$GlcNAc$_2$ (**Q0.M11**), isolated from phCG

Man$_{11}$GlcNAc$_2$ pool

The structural-reporter-group region of the ^{1}H-NMR spectrum of subfraction **Q0.M11** indicated the presence of a mixture of Man$_{11}$GlcNAc$_2$ isomers (Fig. 5d, Scheme 1, Table 1). The Man-**A** H-1 signal at δ 5.100 reflects the presence of Man extensions starting from **Q0.M9-1**; the trace signal at δ 5.404 could indicate very minor amounts of extensions starting from **Q0.M9-2**. In a similar way as discussed for **Q0.M10**, also here N-glycans with additional terminal α(1–3)-linked Man extensions could be eliminated by inspection of 2D TOCSY spectra of **Q0.M11**: no H-1,H-2 correlation was found at δ 5.144/4.23. Compared with the spectrum of **Q0.M10**, that of **Q0.M11** shows various changes in intensities of H-1 signals, related to Man extensions from Man-**4** on (δ ~4.92 and 5.122), and to Man-(α1–2) extensions at Man-(α1–2) residues (δ 5.049 and 5.302).

The Man$_{11}$GlcNAc$_2$ pool was further fractionated by HPAEC (Fig. 6b), and four subfractions were isolated, **Q0.M11-1** (28%), **Q0.M11-2** (31%), **Q0.M11-3** (22%), and **Q0.M11-4** (19%), which were checked by MALDI-TOF-MS to be pure Man$_{11}$GlcNAc$_2$ isomers.

The ^{1}H-NMR spectrum of HPAEC subfraction **Q0.M11-1** is in accordance with structure **Q0.M10-1b** extended with Man-$\mathbf{E_3}$ (Fig. 8a, Scheme 1, Table 1). However, one should keep in mind that for reasons outlined above for **Q0.M10-1a**, a definite choice for the extension of the additional Man residue, at Man-$\mathbf{D_3}$ or at Man-$\mathbf{D_1}$, is not possible.

The ^{1}H-NMR spectrum of HPAEC subfraction **Q0.M11-2** is in accordance with structure **Q0.M10-1b** extended with Man-$\mathbf{D_5}$ or structure **Q0.M10-2** extended with Man-$\mathbf{D_4}$ (Man-**C′** at δ 5.122 and Man-$\mathbf{D_5}$ at δ 4.929) (Fig. 8b, Scheme 1, Table 1). The ^{1}H-NMR data are in good agreement with those reported earlier for Man$_{11}$GlcNAc$_1$ compound IVb [25]. A possible reason for the unusual low intensity of Man-**B** H-1 (δ 5.145) has already been discussed for **Q0.M10-1**. The presence of the additional signal at δ 5.288 could correspond with a Man-$\mathbf{D_1}$ H-1 signal, supporting a Man-(α1–2) extension at Man-$\mathbf{D_1}$ instead of at Man-**C′**. Therefore, it is suggested that **Q0.M11-2** contains besides **Q0.M11-2** also this isomer.

The ^{1}H-NMR spectrum of HPAEC subfraction **Q0.M11-3** is in accordance with structure **Q0.M10-2** extended with Man-$\mathbf{E_5}$ (Fig. 8c, Scheme 1, Table 1). The same intensity problem for Man-**B** as in the previous compound is observed. Comparison of the spectra of **Q0.M11-3** and **Q0.M10-2** learns that the chemical shift of Man-**C′** H-1 (δ 4.911) remains the same, but Man-$\mathbf{D_5}$ becomes (α1–2)-substituted (H-1 at δ 5.121) by Man-$\mathbf{E_5}$. These data are in

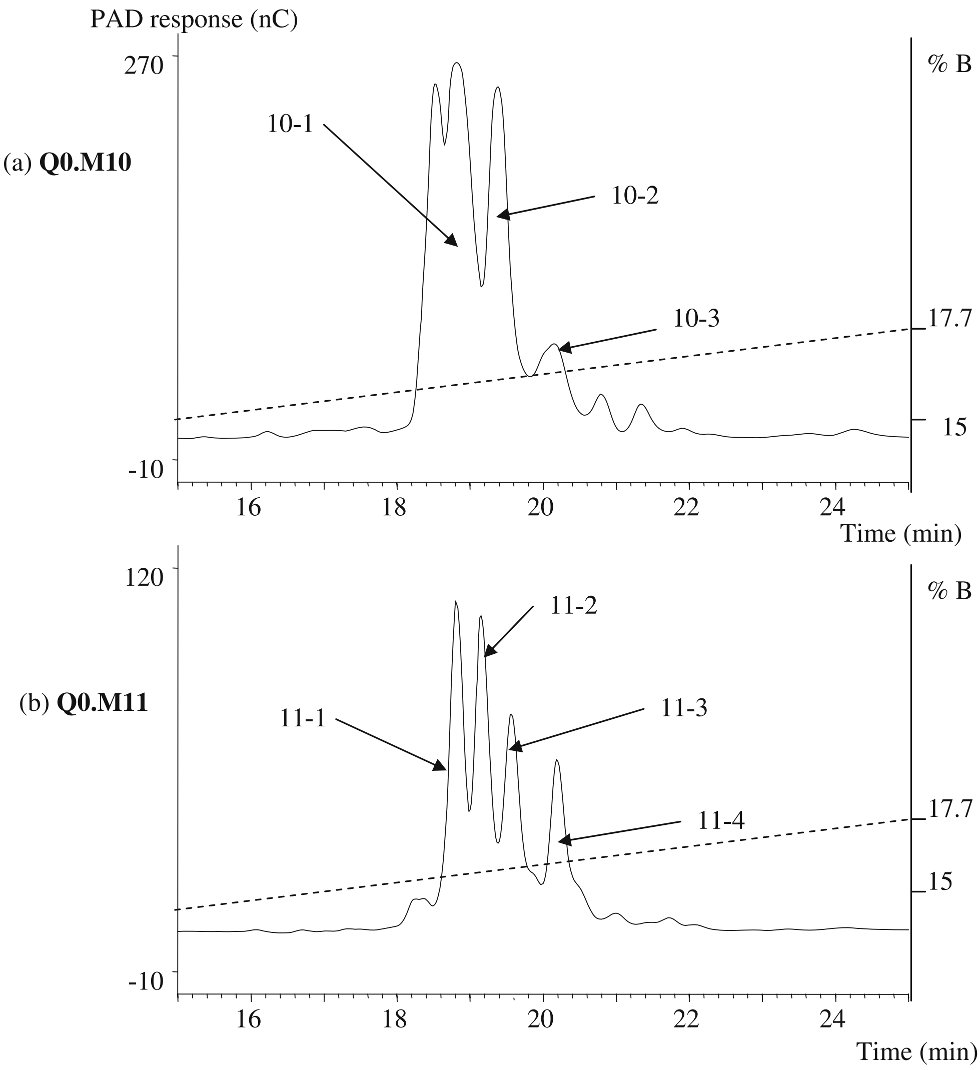

Fig. 6 HPAEC profile using pulsed amperometric detection of (a) fraction **Q0.M10** and (b) fraction **Q0.M11** on a CarboPac PA-1 column. Elutions were carried out with a gradient of sodium acetate in NaOH (see Materials and methods)

accordance with the increase in intensity observed for the H-1 signal corresponding with terminal Man-(α1–2) (δ 5.049) (see also compound IV-C in [25]). The relatively high signal at δ 5.301 could reflect a Man-(α1–2) extension at Man-$\mathbf{D_1}$, as discussed for **Q0.M11-2**.

The ^{1}H-NMR spectrum of HPAEC subfraction **Q0.M11-4** is in accordance with structure **Q0.M10-2** extended with Man-$\mathbf{E_6}$ (Fig. 8d, Scheme 1, Table 1). The (α1–6)-region at δ 4.91 integrates to about three protons, reflecting the sequence Man-$\mathbf{E_6}$-(α1–6)-Man-$\mathbf{D_5}$-(α1–6)-Man-**C′**.

Charged oligosaccharides Q1

The pool of charged N-glycans **Q1** was characterized in terms of molecular mass by MALDI-TOF-MS. In Fig. 2b its negative-ion mode mass spectrum is depicted, showing that the compounds range from Man$_9$*P*GlcNAc$_2$ to Man$_{13}$*P*GlcNAc$_2$. Fractionation of FPLC fraction **Q1** by normal-phase HPLC on Lichrosorb-NH$_2$ gave rise to three subfractions denoted **Q1-1** to **Q1-3** (Fig. 4b), which were analyzed by MALDI-TOF-MS to show that in terms of molecular mass **Q1-1** contained Man$_{9\text{-}11}$*P*GlcNAc$_2$, **Q1-2** Man$_{10\text{-}12}$*P*GlcNAc$_2$, and **Q1-3** Man$_{12–13}$*P*GlcNAc$_2$, dem-

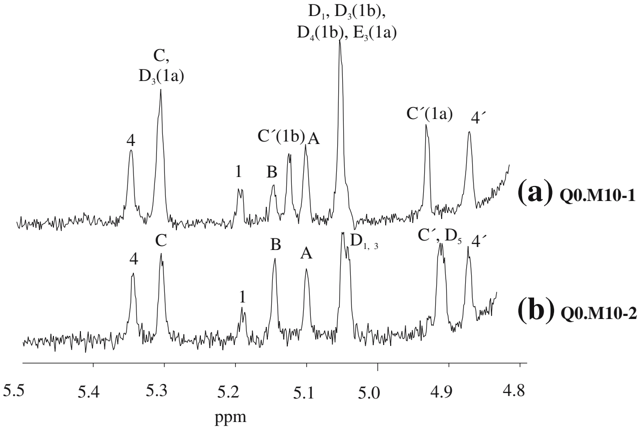

Fig. 7 Anomeric regions of ^{1}H-NMR spectra of subfractions (a) **Q0.M10-1** and (b) **Q0.M10-2**, isolated from phCG

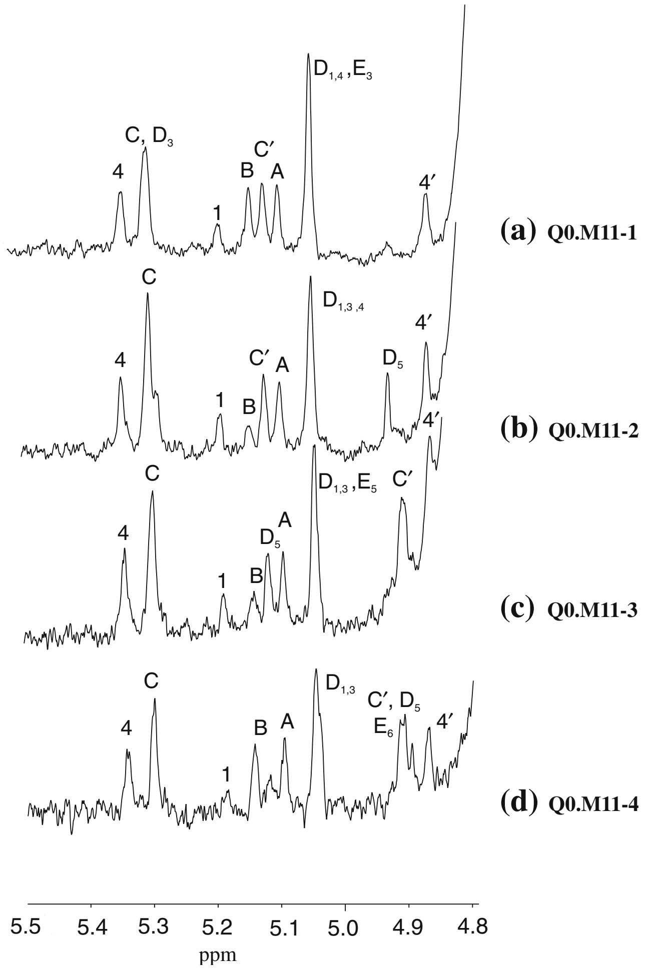

Fig. 8 Anomeric regions of ^{1}H-NMR spectra of subfractions (a) **Q0.M11-1**, (b) **Q0.M11-2**, (c) **Q0.M11-3**, and (d) **Q0.M11-4**, isolated from phCG

onstrating a poor subfractionation. Subfractions **Q1-1**, **Q1-2**, and **Q1-3** were further investigated by HPLC profiling, and **Q1-1** and **Q1-2** by 500-MHz ^{1}H NMR spectroscopy; subfraction **Q1-3** did not contain sufficient material for NMR analysis.

Q1-1 pool (Man$_{9–11}$*P*GlcNAc$_2$)

The HPLC profile (weak anion-exchange Vydac 301 VHP5410 column) of the 2AB-derivatized pool of N-glycans **Q1-1** revealed three peaks, A, B, and C, in the charged region of the chromatogram (Fig. 9a). Treatment of subfraction **Q1-1** with alkaline phosphatase, cleaving only terminal phosphate groups, led to the disappearance of peak C (Fig. 9b), indicating that C corresponds to structures with a dicharged terminal phosphate group that have become neutral after digestion (*P*-Man- → Man-) (data not shown). Positive-ion mode MALDI-TOF-MS of alkaline phosphatase-treated subfraction **Q1-1** demonstrated the presence of neutral Man$_{9–11}$GlcNAc$_2$, in accordance with structures of **Q1-1** before alkaline phosphatase treatment (Man$_{9–11}$*P*GlcNAc$_2$). Treatment of subfraction **Q1-1** with mild acid led to a shift of the position of peak A to that of peak C (Fig. 9c), indicating that A corresponds to structures with an acid-labile monocharged diesterified phosphate group (Man-*P*-Man- → *P*-Man-) [28]. Peak B seems to be a mixture of structures with terminal or diesterified phosphate groups, as deduced from the observation that peak B totally disappears only after both alkaline phosphatase and mild acid incubations. The presence of both diesterified and monoesterified phosphates in **Q1-1** could be due to partial chemical decapping of phosphate during sample handling. Previously, the labilility of Man-*P*-Man-linkages during work-up procedures of *S. cerevisiae* mannoprotein has been mentioned [53].

The structural-reporter-group region of the ^{1}H-NMR spectrum of subfraction **Q1-1** (Fig. 10a, Table 1) is very similar to that of Man$_9$GlcNAc$_2$ (**Q0.M9-1**; Fig. 5b). The two additional “doublets” at δ 5.439 ($J_{H-1,P}$=8.0 Hz) and 5.414 ($J_{H-1,P}$=7.5 Hz) reflect the presence of at least two types of αMan-*P*-groups [54, 55]. In *S. cerevisiae* yeast glycoproteins, phosphate groups are attached to HO6 of Man-**B** and/or Man-**C** within the oligosaccharide chain [53]. As subfraction **Q1-1** contains mainly Man$_{10}$*P*GlcNAc$_2$ (MALDI-TOF-MS), and taking into account the various NMR data, it is suggested that subfraction **Q1-1** contains, at any case, compounds **Q0.M9-1** with Man-*P*-extensions. For

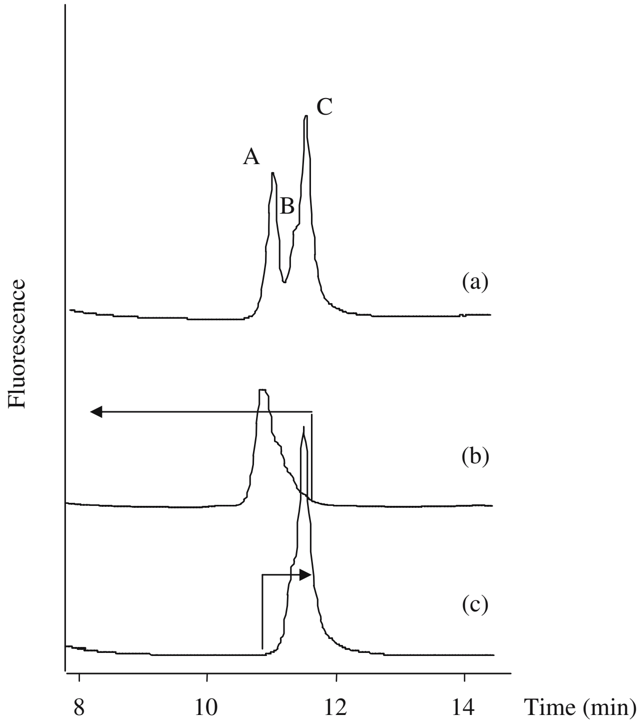

Fig. 9 HPLC profile of the fluorescent 2AB-labeled oligosaccharide mixture **Q1-1** before and after solvolysis on a weak anion-exchange column at a flow rate of 0.4 ml/min and a gradient of ammonium formate, pH 4.4, in acetonitrile. (a) **Q1-1**; (b) **Q1-1** after alkaline phosphatase digestion; (c) **Q1-1** after mild acid hydrolysis

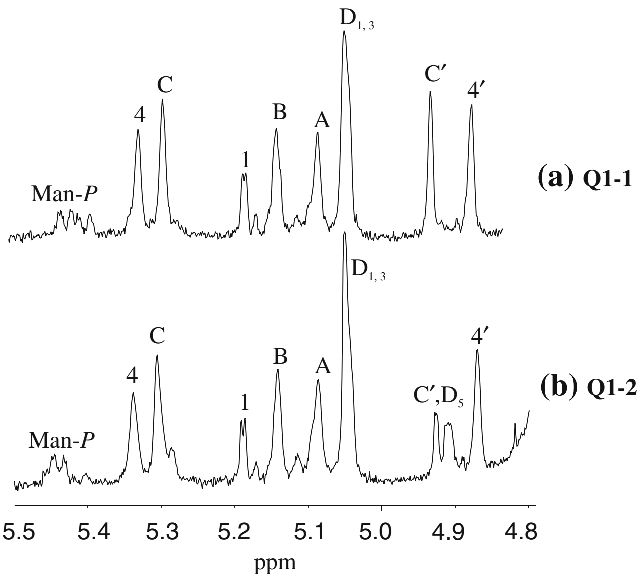

Fig. 10 Anomeric regions of 1D ^{1}H-NMR spectra of charged fractions (a) **Q1-1** and (b) **Q1-2**, isolated from phCG

Man$_x$GlcNAc$_1$ structures, a Man-*P*-extension on Man-**B** has been shown to induce a shift for Man-**A** H-1 of $\Delta\delta = -0.008$ (compare structure B in [43] with structure I in [53]); no shifts are observed for Man-**B** and Man-**D$_3$** H-1. Comparison of the Man-**A** H-1 signals in **Q0.M9-1** (δ 5.099) and in **Q1-1** (δ 5.086) shows a similar upfield shift ($\Delta\delta = -0.013$), thereby supporting the presence of a component **Q0.M9-1** mannophosphorylated at HO6 of Man-**B**; in Man*P*Man$_9$GlcNAc$_2$, Man-**D$_3$** H-1 is slightly ($\Delta\delta = -0.005$) influenced. For Man$_x$GlcNAc$_1$ structures, a Man-*P*-extension on Man-**C** caused an upfield shift of Man-**C** H-1 of $\Delta\delta = -0.019$ (compare structure B in [43] with structure IV in [53]). Such a shift is not observed comparing the Man-**C** H-1 values in **Q0.M9-1** and **Q1-1**. As already discussed above, increments detected for ^{1}H-NMR values of the Man$_x$GlcNAc$_1$ series seems to be not always transferable to the Man$_x$GlcNAc$_2$ series, and problems were detected with respect to the Man-**D$_1$**-Man-**C**-Man-**4** sequence. Having two clear αMan-*P* H-1 signals in the ^{1}H-NMR spectrum, it is therefore hypothesized that a component **Q0.M9-1** mannophosphorylated at HO6 of Man-**C** is also present. The relatively low intensities of the two αMan-*P* H-1 signals support the presence of Man$_{9-11}$GlcNAc$_2$ structures, only phosphorylated on one of the two residues. The small H-1 signal at δ 5.120 (Man-**D$_4$**-(α1–2)-Man-**C′** segment) suggests at any case the presence of a phospho-extended structure **Q0.M10-1b**.

Q1-2 and **Q1-3** pools (Man$_{10-12}$*P*GlcNAc$_2$ and Man$_{12-13}$*P*GlcNAc$_2$)

The HPLC profiles of the 2AB-derivatized pools of N-glycans **Q1-2** and **Q1-3** were similar to that of **Q1-1**, and behaved in the same way when incubated with alkaline phosphatase or mild acid. Consequently, also subfractions **Q1-2** and **Q1-3** contain mixtures of structures with *P*-Man and Man-*P*-Man elements.

The structural-reporter-group region of the ^{1}H-NMR spectrum of subfraction **Q1-2** (Fig. 10b, Table 1) shows a major characteristic doublet at δ 5.439 ($J_{\mathrm{H-1,P}}$=8.0 Hz) and two minor ones at δ 5.411 ($J_{\mathrm{H-1,P}}$=7.5 Hz) and δ 5.450 ($J_{\mathrm{H-1,P}}$=8.0 Hz), in agreement with the presence of αMan-*P*-groups [54, 55]. As indicated by MALDI-TOF-MS, subfraction **Q1-2** contains mainly Man$_{11}$*P*GlcNAc$_2$. In view of the broad H-1 signal at δ 4.912, also present in the ^{1}H-NMR spectrum of **Q0.M10-2** (Man- **C′** and Man-**D$_5$**), it is suggested that **Q1-2** contains at least a Man-*P*-extension of **Q0.M10-2**. The Man-**A** H-1 signal at δ 5.086 supports a mannophosphorylation at HO6 of Man-**B**. The relative low intensities of the three αMan-*P* H-1 signals support the presence of Man$_{10-12}$GlcNAc$_2$ structures, only phosphorylated on one of the two residues. The signals at δ 5.285, 5.122, and 4.929 correspond with Man-**C**, Man-**C′**, and Man-**D$_5$** signals also present in **Q0.M11-2**.

Charged oligosaccharides Q2

The amount of the pool of charged N-glycans of **Q2** was not sufficient for NMR studies or HPLC subfractionation. To gain some information about the components of the fraction, weak-anion HPLC profiling was conducted after 2AB derivatization. The chromatogram showed two peak

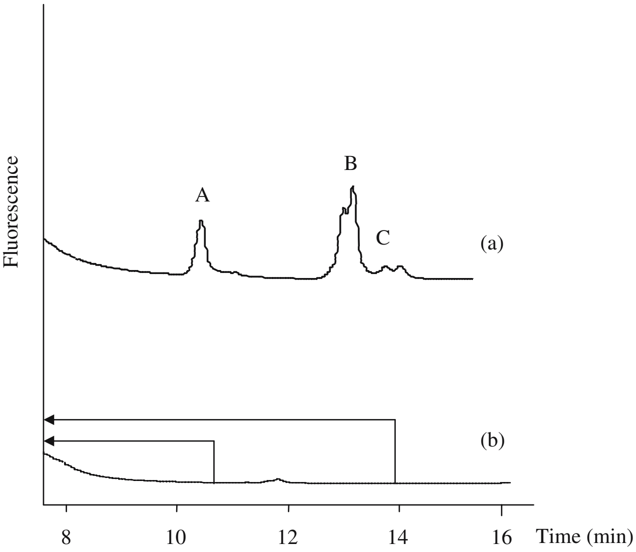

Fig. 11 HPLC profile of the fluorescent 2AB-labeled oligosaccharide mixture **Q2** before and after solvolysis on a weak anion-exchange column at a flow rate of 0.4 ml/min and a gradient of ammonium formate, pH 4.4, in acetonitrile. (a) **Q2** and **Q2** after alkaline phosphatase digestion; (b) **Q2** after mild acid hydrolysis and alkaline phosphatase digestion

Table 2 Carbohydrate chains occurring in phCG produced in batch I and batch II

	Batch I		Batch II	
	α	β	α	β
$Man_8GlcNAc_2$	17	18	4	5
$Man_9GlcNAc_2$	39	41	32	24
$Man_{10}GlcNAc_2$	30	24	37	36
$Man_{11}GlcNAc_2$	11	13	23	29
$Man_{12}GlcNAc_2$	3	4	4	6

Results are based on peak areas of the 2AB-chromatograms

areas A and B + C in the acidic region, with a relevant difference in retention time (Fig. 11). After treatment with alkaline phosphatase, the HPLC peak pattern of **Q2** did not change, indicating the absence of *P*-Man-elements. Mild acid hydrolysis followed by an alkaline phosphatase digestion resulted in the complete disappearance of the charged components' peaks. Taking into account their retention times, it is speculated that peak A reflects glycans with one terminal Man-*P*-Man motif, and peaks B + C glycans with two terminal Man-*P*-Man motifs [28].

Profiling studies of α-phCG and β-phCG from phGC batches I and II

To compare the influence of the culturing medium on the N-glycosylation pattern of *P. pastoris* expressed hCG (phCG), two protocols were applied, yielding phCG batch I and phCG batch II. For batch I, ammonia was used as nitrogen source; for batch II, ammonium sulfate. Both batches were subjected to reduction, carboxymethylation, and separation of the α- and β-subunits on Superdex G75. MALDI-TOF-MS of α-phCG showed a molecular mass of 15 kDa, corresponding to about 11 kDa of protein backbone and 2 N-glycans of a mass in the range of 2 kDa each. For β-hCG these values are 19 kDa, about 15 kDa, and about 4 kDa reflecting 2 N-glycans, respectively.

The 4 samples were digested with PNGase F, and SDS-PAGE was used to verify the completeness of the de-N-glycosylation. The released free N-glycans of α-phCG I, β-phCG I, α-phCG II, and β-phCG II were converted into their 2AB-labeled derivatives, and analyzed by MALDI-TOF-MS and HPLC.

As is evident from Table 2, the same neutral high mannose-type structures were present in both batches, but in different proportions. α- and β-phCG batch I contained higher amounts of $Man_8GlcNAc_2$ and $Man_9GlcNAc_2$ than α- and β-phCG batch II. The reverse held for $Man_{10}GlcNAc_2$ and Man_{11}-$GlcNAc_2$. In both batches, $Man_{12}GlcNAc_2$ was a minor compound. Significant differences in size of the glycans on the subunits of a given batch were not observed. The profiles of the charged glycans showed identical patterns for the two batches and their subunits. It seems that the conditions used for the preparation of batch II induces more biosynthetic processing than those used for batch I.

Discussion

Structural analysis of the N-glycans of hCG expressed in the methylotrophic yeast *Pichia pastoris* has resulted in the identification of a pool of 80% neutral N-glycans and 20% charged (phosphorylated) N-glycans. Neutral N-glycans could be detected in the range of $Man_8GlcNAc_2$ to $Man_{15}GlcNAc_2$. Based on MS, HPLC and NMR studies, for 10 components structures could be elucidated. Phosphorylated N-glycans were found in the range of $Man_9PGlcNAc_2$ to $Man_{13}PGlcNAc_2$. Both Man-*P*-Man- and *P*-Man-elements were detected, but probably *P*-Man-elements were introduced during work-up. The majority of the N-glycans contained 9 to 10 Man residues, independent on the chosen culturing process, whereby $Man_9GlcNAc_2$ nearly only represents the typical yeast isomer. However, culturing conditions did influence the molar ratio within $Man_{8-12}GlcNAc_2$. It should be noted that previous NMR structural studies of yeast glycoprotein N-glycans were always carried out on $Man_x(P_y)GlcNAc_1$ compounds; in the present investigation NMR data of $Man_x(P_y)GlcNAc_2$ compounds are presented.

As urinary β-hCG contains O-linked glycans, and in view of the fact that *P. pastoris*-expressed glycoproteins can be O-mannosylated [29–32], β-phCG was checked for O-mannosylation. Monosaccharide analysis performed on N-deglycosylated phCG did not show any sugar constituent. In addition, MALDI-TOF-MS of β-phCG showed a molecular mass of 19 kDa, corresponding to about 15 kDa of protein backbone and 2 N-glycans of a mass in the range of 2 kDa each.

In conclusion, as expected, in the *P. pastoris*-expressed hCG (phCG), the glycosylation pattern is totally different from that of urinary hCG. However, earlier studies have already shown that, like urinary hCG, phCG is biologically active [23]. Both glycohormones show the same receptor-binding potential, and stimulate testosterone production by mouse Leydig cells and progesterone production by MA-10 cells. The present study on non-O-glycosylated phCG also shows that the O-glycosylation of β-hCG seems to have little influence on receptor binding and signal transduction, in accordance with earlier studies on urinary hCG [56]. In several studies, the importance of the N-glycosylation at Asn52 of urinary α-hCG for steroidogenic activity has been shown [56, 57], and it has been postulated that the bulky and extended glycan at this site could have a function in inducing and stabilizing a conformational change in hCG upon binding to the receptor [58]. It is suggested that the high-mannose-type *N*-glycans on αAsn52 in phCG accomplish the same function.

Acknowledgment This research has been financially supported by the Council for Chemical Sciences of the Netherlands Organization for Scientific Research (CW-NWO).

References

1. Talwar, G.P.: Human chorionic gonadotropin and ovarian and placental steroidogenesis. J. Steroid Biochem. **11**, 27–34 (1979)
2. Endo, T., Yamashita, K., Tachibana, Y., Tojo, S., Kobata, A.: Structures of the asparagine-linked sugar chains of human chorionic gonadotropin. J. Biochem. (Tokyo) **85**, 669–679 (1979)
3. Blithe, D.L.: Carbohydrate composition of the α-subunit of human chorionic gonadotropin (hCGα) and the free α molecules produced in pregnancy: most free α and some combined hCGα molecules are fucosylated. Endocrinology **126**, 2788–2799 (1990)
4. Weisshaar, G., Hiyama, J., Renwick, A.G.C.: Site-specific *N*-glycosylation of human chorionic gonadotropin, Structural analysis of glycopeptides by one- and two-dimensional ^{1}H NMR spectroscopy. Glycobiology **1**, 393–404 (1991)
5. Damm, J.B.L., Voshol, H., Hård, K., Kamerling, J.P., van Dedem, G.W.K., Vliegenthart, J.F.G.: The β-subunit of human chorionic gonadotropin contains *N*-glycosidic trisialo tri- and tri′-antennary carbohydrate chains. Glycoconj. J. **5**, 221–233 (1988)
6. Damm, J.B.L., Kamerling, J.P., van Dedem, G.W.K., Vliegenthart, J.F.G.: A general strategy for the isolation of carbohydrate chains from N-,O-glycoproteins and its application to human chorionic gonadotrophin. Glycoconj. J. **4**, 129–144 (1987)
7. Amano, J., Nishimura, R., Mochizuki, M., Kobata, A.: Comparative study of the mucin-type sugar chains of human chorionic gonadotropin present in the urine of patients with trophoblastic diseases and healthy pregnant women. J. Biol. Chem. **263**, 1157–1165 (1988)
8. Liu, C.L., Bowers, L.D.: Mass spectrometry characterisation of the beta-subunit of human chorionic gonadotropin. J. Mass Spectrom. **32**, 33–42 (1997)
9. Cole, L.A.: Distribution of O-linked sugar units on hCG and its free alpha-subunit. Mol. Cell. Endocrinol. **50**, 45–57 (1987)
10. Bielinska, M., Boime, I.: The glycoprotein hormone family: structure and function of the carbohydrate chains. In: Montreuil, J., Vliegenthart, J.F.G., Schachter, H. (eds.) Glycoproteins, Vol. 29a, pp. 565–587. New Comprehensive Biochemistry, Elsevier Science BV, Amsterdam, The Netherlands (1995)
11. Kamerling, J.P., Hård, K., Vliegenthart, J.F.G.: Structural analysis of carbohydrate chains of native and recombinant-DNA glycoproteins. In: Crommelin, D.J.A., Schellekens, H. (eds.) Developments in Biotherapy, Vol. 1, From Clone to Clinic, pp. 295–304. Kluwer Academic Publishers, Dordrecht, The Netherlands (1990)
12. Gervais, A., Hammel, Y.-A., Pelloux, S., Lepage, P., Baer, G., Carte, N., Sorokine, O., Strub, J.-M., Koerner, R., Leize, E., Van Dorsselaer, A.: Glycosylation of human recombinant gonadotrophins: characterization and batch-to-batch consistency. Glycobiology **13**, 179–189 (2003)
13. Lustbader, J.W., Birken, S., Pollak, S., Pound, A., Chait, B.T., Mirza, U.A., Ramnarain, S., Canfield, R.E., Brown, J.M.: Expression of human chorionic gonadotropin uniformly labeled with NMR isotopes in Chinese hamster ovary cells: An advance toward rapid determination of glycoprotein structures. J. Biomol. NMR **7**, 295–304 (1996)
14. Chen, W., Shen, Q.X., Bahl, O.P.: Carbohydrate variant of the recombinant beta-subunit of human choriogonadotropin expressed in baculovirus expression system. J. Biol. Chem. **266**, 4081–4087 (1991)
15. Chen, W., Bahl, O.P.: Recombinant carbohydrate variant of human choriogonadotropin beta-subunit (hCGbeta) descarboxyl terminus (115–145). Expression and characterization of carboxyl-terminal deletion mutant of hCG beta in the baculovirus system. J. Biol. Chem. **266**, 6246–6251 (1991)
16. Chen, W., Bahl, O.P.: Recombinant carbohydrate and selenomethionyl variants of human choriogonadotropin. J. Biol. Chem. **266**, 8192–8197 (1991)
17. Jung, E., Williams, K.L.: The production of recombinant glycoproteins with special reference to simple eukaryotes including *Dictyostelium discoideum*. Biotechnol. Appl. Biochem. **25**, 3–8 (1997)
18. Linskens, M.H.K., Grootenhuis, P.D.J., Blaauw, M., Huisman-de Winkel, B., van Ravenstein, A., van Haastert, P.J.M., Heikoop, J. C.: Random mutagenesis and screening of complex glycoproteins: expression of human gonadotropins in *Dictyostelium discoideum*. FASEB J. **13**, 639–645 (1999)
19. Peters, B.P., Krzesicki, R.F., Hartle, R.J., Perini, F., Ruddon, R. W.: A kinetic comparison of the processing and secretion of the alpha beta dimer and the uncombined alpha and beta subunits of chorionic gonadotropin synthetized by human choriocarcinoma cells. J. Biol. Chem. **258**, 15123–15130 (1984)
20. Cole, L.A., Kroll, T.D., Ruddon, R.W., Hussa, R.O.: Differential occurrence of free beta and free alpha subunits of human chorionic gonadotropin (hCG) in pregnancy sera. J. Clin. Endocrinol. Metab. **58**, 1200–1202 (1984)
21. Lustbader, J., Birken, S., Pollak, S., Levinson, L., Berstine, E., Hsiung, N., Cornfield, R.: Characterization of the expression products of recombinant human choriogonadotropin and subunits. J. Biol. Chem. **262**, 14204–14212 (1987)
22. Sen Gupta, C., Dighe, R.R.: Hyperexpression of biologically active human chorionic gonadotropin using the methylotropic yeast, *Pichia pastoris*. J. Mol. Endocrinol. **22**, 273–283 (1999)
23. Gadkari, R., Deshpande, R., Dighe, R.R.: Hyperexpression and purification of biologically active human luteinizing hormone and human chorionic gonadotropin using the methylotrophic yeast, *Pichia pastoris*. Protein Expr. Purif. **32**, 175–184 (2003)
24. Grinna, L.S., Tschopp, J.F.: Size distribution and general structural features of N-linked oligosaccharides from the methylotrophic yeast, *Pichia pastoris*. Yeast **5**, 107–115 (1989)
25. Trimble, R.B., Atkinson, P.H., Tschopp, J.F., Townsend, R.R., Maley, F.: Structure of oligosaccharides on *Saccharomyces SUC2* invertase secreted by the methylotrophic yeast *Pichia pastoris*. J. Biol. Chem. **266**, 22807–22817 (1991)
26. Miele, R.G., Nilsen, S.L., Brito, T., Bretthauer, R.K., Castellino, F.J.: Glycosylation properties of the *Pichia pastoris*-expressed recombinant kringle 2 domain of tissue-type plasminogen activator. Biotechnol. Appl. Biochem. **25**, 151–157 (1997)

27. Gemmill, T.R., Trimble, R.B.: Overview of N- and O-linked oligosaccharide structures found in various yeast species. Biochim. Biophys. Acta **1426**, 227–237 (1999)
28. Hirose, M., Kameyama, S., Ohi, H.: Characterization of N-linked oligosaccharides attached to recombinant human antithrombin expressed in the yeast *Pichia pastoris*. Yeast **19**, 1191–1202 (2002)
29. Boraston, A.B., Sandercock, L.E., Warren, R.A.J., Kilburn, D.G.: O-Glycosylation of a recombinant carbohydrate-binding module mutant secreted by *Pichia pastoris*. J. Mol. Microbiol. Biotechnol. **5**, 29–36 (2003)
30. Cereghino, J.L., Cregg, J.M.: Heterologous protein expression in the methylotrophic yeast *Pichia pastoris*. FEMS Microbiol. Rev. **24**, 45–66 (2000)
31. Letourneur, O., Gervasi, G., Gaïa, S., Pagès, J., Watelet, B., Jolivet, M.: Characterization of *Toxoplasma gondii* surface antigen I (SAGI) secreted from *Pichia pastoris*: evidence of hyper O-glycosylation. Biotechnol. Appl. Biochem. **33**, 35–45 (2001)
32. González, L.J., Cremata, J.A., Guanche, Y., Ramos, Y., Triguero, A., Cabrera, G., Montesino, R., Huerta, V., Pons, T., Boué, O., Farnós, O., Rodríguez, M.: The cattle tick antigen, Bm95, expressed in *Pichia pastoris* contains short chains of N- and O-glycans. Arch. Biochem. Biophys. **432**, 205–211 (2004)
33. Kamerling, J.P., Vliegenthart, J.F.G.: Carbohydrates. In: Lawson, A.M. (ed.) Clinical Biochemistry—Principles, Methods, Applications, Vol 1, Mass Spectrometry, pp. 175–263. Walter de Gruyter, Berlin, Germany (1989)
34. Packer, N.H., Lawson, M.A., Jardine, D.R., Redmond, J.W.: A general approach to desalting oligosaccharides released from glycoproteins. Glycoconj. J. **15**, 737–747 (1988)
35. Thieme, T.R., Ballou, C.E.: Nature of the phosphodiester linkage of the phosphomannan from the yeast *Kloeckera brevis*. Biochemistry **10**, 4121–4129 (1971)
36. Bigge, J.C., Patel, T.P., Bruce, J.A., Goulding, P.N., Charles, S. M., Parekh, R.B.: Nonselective and efficient fluorescent labeling of glycans using 2-aminobenzamide and anthranilic acid. Anal. Biochem. **230**, 229–238 (1995)
37. Stroop, C.J.M., Weber, W., Gerwig, G.J., Nimtz, M., Kamerling, J.P., Vliegenthart, J.F.G.: Characterization of the carbohydrate chains of the secreted form of the human epidermal growth factor receptor. Glycobiology **10**, 901–917 (2000)
38. Narui, T., Iwata, S., Takahashi, K., Shibata, S.: Partial hydrolysis of α-D-glucans with acid in the presence of 1,1,3,3-tetramethylurea. Carbohydr. Res. **170**, 269–273 (1987)
39. Guile, G.R., Rudd, P.M., Wing, D.R., Prime, S.B., Dwek, R.A.: A rapid high-resolution high-performance liquid chromatographic method for separating glycan mixtures and analyzing oligosaccharide profiles. Anal. Biochem. **240**, 210–226 (1996)
40. Papac, D.I., Briggs, J.B., Chin, E.T., Jones, A.J.S.: A high-throughput microscale method to release N-linked oligosaccharides from glycoproteins for matrix-assisted laser desorption/ionization time-of-flight mass spectrometric analysis. Glycobiology **8**, 445–454 (1998)
41. Vliegenthart, J.F.G., Dorland, L., van Halbeek, H.: High-resolution, ^{1}H-nuclear magnetic resonance spectroscopy as a tool in the structural analysis of carbohydrates related to glycoproteins. Adv. Carbohydr. Chem. Biochem. **41**, 209–374 (1983)
42. Hård, K., van Zadelhoff, G., Moonen, P., Kamerling, J.P., Vliegenthart, J.F.G.: The Asn-linked carbohydrate chains of human Tamm-Horsfall glycoprotein of one male. Novel sulfated and novel *N*-acetylgalactosamine-containing N-linked carbohydrate chains. Eur. J. Biochem. **209**, 895–915 (1992)
43. Hernández, L.M., Ballou, L., Alvarado, E., Gillece-Castro, B.L., Burlingame, A.L., Ballou, C.E.: A new *Saccharomyces cerevisiae mnn* mutant N-linked oligosaccharide structure. J. Biol. Chem. **264**, 11849–11856 (1989)
44. Koles, K., van Berkel, P.H.C., Pieper, F.R., Nuijens, J.H., Mannesse, M.L.M., Vliegenthart, J.F.G., Kamerling, J.P.: N- and O-glycans of recombinant human C1 inhibitor expressed in the milk of transgenic rabbits. Glycobiology **14**, 51–64 (2004)
45. Michalski, J.-C., Haeuw, J.-F., Wieruszeski, J.-M., Montreuil, J., Strecker, G.: *In vitro* hydrolysis of oligomannosyl oligosaccharides by the lysosomal α-D-mannosidases. Eur. J. Biochem. **189**, 369–379 (1990)
46. Tseneklidou-Stoeter, D., Gerwig, G.J., Kamerling, J.P., Spindler, K.-D.: Characterization of N-linked carbohydrate chains of the crayfish, *Astacus leptodactylus* hemocyanin. Biol. Chem. Hoppe-Seyler **376**, 531–537 (1995)
47. Byrd, J.C., Tarentino, A.L., Maley, F., Atkinson, P.H., Trimble, R. B.: Glycoprotein synthesis in yeast; identification of Man$_{8}$-GlcNAc$_2$ as an essential intermediate in oligosaccharide processing. J. Biol. Chem. **257**, 14657–14666 (1982)
48. De Waard, P., Kamerling, J.P., van Halbeek, H., Vliegenthart, J.F. G., Broertjes, J.S.S.: Characterization of N-linked gluco-oligomannose type of carbohydrate chains of glycoproteins from the ovary of the starfish *Asterias rubens* (L.). Eur. J. Biochem. **168**, 679–685 (1987)
49. Trimble, R.B., Atkinson, P.H.: Structure of yeast external invertase Man$_{8-14}$GlcNAc processing intermediates by 500-megahertz ^{1}H NMR spectroscopy. J. Biol. Chem. **261**, 9815–9824 (1986)
50. Cohen, R.E., Ballou, C.E.: Linkage and sequence analysis of mannose-rich glycoprotein core oligosaccharides by proton nuclear magnetic resonance spectroscopy. Biochemistry **19**, 4345–4358 (1980)
51. Hardy, M.R., Townsend, R.R.: Separation of fucosylated oligosaccharides using high-pH anion-exchange chromatography with pulsed-amperometric detection. Carbohydr. Res. **188**, 1–7 (1989)
52. Hernández, L.M., Ballou, L., Ballou, C.E.: Separation of yeast asparagine-linked oligosaccharides by high-performance anion-exchange chromatography. Carbohydr. Res. **203**, 1–11 (1990)
53. Hernández, L.M., Ballou, L., Alvarado, E., Tsai, P., Ballou, C.E.: Structure of the phosphorylated N-linked oligosaccharides from the *mnn9* and *mnn10* mutants of *Saccharomyces cerevisiae*. J. Biol. Chem. **264**, 13648–13659 (1989)
54. Hernández, L.M., Olivero, I., Alvarado, E., Larriba, G.: Oligosaccharide structures of the major exoglucanase secreted by *Saccharomyces cerevisiae*. Biochemistry **31**, 9823–9831 (1992)
55. De Waard, P., Vliegenthart, J.F.G., Kozutsumi, Y., Kawasaki, T., Yamashina, I.: Structural studies on phosphorylated oligosaccharides derived from yeast mannan by 1H(31P) relayed spin-echo difference spectroscopy (RESED). J. Biol. Chem. **264**, 12141-12144 (1989)
56. Matzuk, M.M., Hsueh, A.J.W., Lapolt, P., Tsafriri, A., Keene, J.L., Boime, I.: The biological role of the carboxy-terminal extension of human chorionic gonadotropin β-subunit. Endocrinology **126**, 376–383 (1990)
57. Sairam, M.R., Jiang, L.G.: Comparison of the biological and immunological properties of glycosylation deficient human chorionic gonadotropin variants produced by site directed mutagenesis and chemical deglycosylation. Mol. Cell. Endocrinol. **85**, 227–235 (1992)
58. Erbel, P.J., Haseley, S.R., Kamerling, J.P., Vliegenthart, J.F.G.: Studies on the relevance of the glycan at Asn-52 of the α-subunit of human chorionic gonadotropin in the αβ dimer. Biochem. J. **364**, 485–495 (2002)